
Since January 2020 Elsevier has created a COVID-19 resource centre with free information in English and Mandarin on the novel coronavirus COVID-19. The COVID-19 resource centre is hosted on Elsevier Connect, the company's public news and information website.

*Microbial Pathogenesis* 1995; **18**: 253–267

# Mouse neuropathogenic poliovirus strains cause damage in the central nervous system distinct from poliomyelitis

**Matthias Gromeier*, Hui-Hua Lu, Eckard Wimmer**

*Department of Molecular Genetics and Microbiology, School of Medicine, State University of New York at Stony Brook, Stony Brook, N.Y. 11794–8621*

(Received December 27, 1994, Accepted in revised form February 23, 1995)

Gromeier, M. (Department of Molecular Genetics and Microbiology, School of Medicine, State University of New York, Stony Brook, N.Y. 11794–8621, U.S.A.), H.-H. Lu and E. Wimmer, Mouse neuropathogenic poliovirus strains cause damage in the central nervous system distinct from poliomyelitis. *Microbial Pathogenesis* 1995; **18**: 253–267.

Poliomyelitis as a consequence of poliovirus infection is observed only in primates. Despite a host range restricted to primates, experimental infection of rodents with certain genetically well defined poliovirus strains produces neurological disease. The outcome of infection of mice with mouse-adapted poliovirus strains has been described previously mainly in terms of paralysis and death, and it was generally assumed that these strains produce the same disease syndromes in normal mice and in mice transgenic for the human poliovirus receptor (*h*PVR-*tg* mice). We report a comparison of the clinical course and the histopathological features of neurological disease resulting from intracerebral virus inoculation in normal mice with those of murine poliomyelitis in *h*PVR-*tg* mice. The consistent pattern of clinical deficits in poliomyelitic transgenic mice contrasted with highly variable neurologic disease that developed in mice infected with different mouse-adapted polioviruses. Histopathological analysis showed a diffuse encephalomyelitis induced by specific poliovirus serotype 2 isolates in normal mice, that affected neuronal cell populations without discrimination, whereas in *h*PVR-*tg* animals, damage was restricted to spinal motor neurons. Mouse neurovirulent strains of poliovirus type 2 differed from mouse neurovirulent poliovirus type 1 derivatives in their ability to induce CNS lesions. Our findings indicate that the characteristic clinical appearance and highly specific histopathological features of poliomyelitis are mediated by the *h*PVR. Our data lead us to conclude that the tissue tropism of mouse-adapted poliovirus strains in normal mice is fundamentally different from that of poliovirus in *h*PVR-*tg* mice and primates, and that this is indicative of an as yet unknown mechanism of adsorption and uptake of the virus into cells of the murine CNS.

## Introduction

Poliomyelitis is a rare neurological complication of primate infection with poliovirus (PV), a member of the Picornavirus family, genus Enterovirus. Ingestion of virulent particles results in intestinal uptake, presumably through M-cells,[1] initial viral replication in subjacent lymphatic tissue, spread to deeper cervical and mesenteric

*Author to whom correspondence should be addressed.

0882-4010/95/040253+15 $08.00/0

lymph nodes (lymphatic phase), and ultimately entry of the virus into the bloodstream (viremic phase).[2] The latter is a prerequisite for passage of the blood brain barrier[3] and subsequent lytic infection of motor neurons.

Only a small proportion of PV infections lead to a distinctive neurological syndrome that ranges in severity from transient flaccid monoparesis to progressive flaccid paraplegia with respiratory impairment and sometimes bulbar involvement.[4] The hallmark of poliomyelitis histopathology is selective damage to anterior horn motor neurons along the entire spinal cord. Spinal neurons outside the motor neuron system are characteristically spared,[5] in spite of their close anatomical relationship to the target of polioviral attack.

The predominant molecular determinant of PV tropism is the *h*PVR.[6,7] The nucleotide sequence of *h*PVR identified it to be a member of the immunoglobulin superfamily, whose four mRNA isoforms are the result of alternative splicing events, and give rise to different receptor molecules.[6,8] *h*PVR$\alpha$ and *h*PVR$\delta$ are integral membrane proteins with divergent cytoplasmatic domains, whereas *h*PVR$\beta$ and *h*PVR$\gamma$ are secreted molecules lacking the putative transmembrane domain.[6] The *h*PVR is a highly glycosylated protein with an apparent molecular weight of 80kDa.[9] The animal model for poliomyelitis in *h*PVR-*tg* mice showed PV-induced damage of comparable anatomical distribution as in primates,[10,11] an observation confirming views of the *h*PVR as the critical determinant conferring PV susceptibility.

Unexpectedly, *h*PVR mRNA and *h*PVR-related proteins were shown to be present in a wide variety of tissue homogenates not known to be sites of PV replication,[7,10] an observation suggesting additional limiting factors of PV susceptibility. mRNAs specifying the simian[12] and murine[13] homologues to *h*PVR have been isolated, but only the monkey-specific PVR can promote PV infection.[12]

Attempts to use rodents as possible models of PV-induced disease resulted in the isolation of mouse-neurovirulent (*mn*) strains. A 1937 PV serotype 2 field isolate from Lansing, Michigan, [PV2(L)], which caused a syndrome described as 'polioencephalitis' upon intracerebral injection in the cotton rat,[14] provided the first system of PV encephalitogenesis in the wild type (*wt*) mouse.[15] Histopathological analyses of murine infection with the rodent-passaged PV2(L) isolate described a pattern of damage in accordance with concepts of primate poliomyelitis.[16]

A structural element conferring mouse neurovirulence to PV2(L) was determined to map in the capsid region.[17] Sufficient in causing this effect was a segment within the BC-loop of VP1 since mouse avirulent PV type 1 (Mahoney) [PV1(M)], after transposition of the Lansing BC-loop, caused neurological disease in mice.[18,19] Surprisingly, point mutations in distant regions of VP1 and VP2 could be shown to exert a *mn* phenotype.[20,21] The histopathological features of neurological disease caused by these genetically well defined *mn* PV strains have not been reported thus far.

In addition to the selection of *wt* PV strains expressing a *mn* phenotype in mice, attenuated PV strains with a mouse host range phenotype but reduced neurovirulence have also been described [PV type 2, strain W2[22]]. The attenuated (*att*) phenotype of PV2(W2) is reminiscent of the Sabin strains of PV that express an *att* phenotype for primates.[23]

The genetic determinants of viral neurotropism have been studied in several viral systems. Most frequently, these determinants mapped to the envelope gene; examples are the alphaviruses Sindbis virus[24,25] and Semliki Forest virus,[26] the flaviviruses tick-borne encephalitis virus[27] and Dengue virus,[28] influenza virus,[29] rabies virus,[30] the ecotropic murine retroviruses,[31] and murine coronaviruses.[31] Similarly, structural elements of the capsid influence reovirus neurotropism,[32] and Theiler's virus neurovirulent potential.[34] Whether altered neurotropism is secondary to changes in the

interaction of viral surface proteins with cellular recognition molecules remains an open question.[35,36]

We have infected Swiss-Webster-, and ICR-mice with a variety of *mn* virus isolates of different serotypical origin. Type 2 strains PV2(L), PV2(MEF-1), a recent PV2 isolate from India (IND), and PV2(W2) caused a fatal diffuse encephalomyelitis in these mice with considerable differences in intensity between individual viral strains. PV1(LS-a), a mouse-adapted derivative of PV1(M),[37] caused a characteristic non-progressive panmyelitic syndrome. We have also studied the histopathology of murine infection with PV1(M), carrying a single mutation in position 54 of capsid protein VP1 that we constructed according to a published report.[21]

Infections with each of these strains did not follow the stereotypic course of predictable progression seen in PV-induced poliomyelitis in *h*PVR-*tg* ICR-mice. Syndromes with distinct and consistent features followed intracerebral infection with each group of strains. These syndromes could be separately characterized and distinguished from *h*PVR-mediated poliomyelitis, on both clinical and histopathological grounds.

## Materials and methods

***Poliovirus isolates and experimental animals.*** PV1(M) was propagated in HeLa cell cultures and isolated and purified according to standard procedures.[38] PV2(W2), a rodent adapted serotype 2 strain[39] was kindly provided by B. Jubelt (SUNY Medical Center, Syracuse, NY, U.S.A). PV1(LS-a) was originally obtained after serial passages of PV1(M) through monkeys, tissue cultures and the murine spinal cord.[37] PV2(L) is a rodent passaged field isolate from a fatal case of poliomyelitis in Lansing, MI,[15] PV2(MEF-1) is a field isolate from 1941 sampled in Cairo, Egypt,[40] and PV2(IND) is an Indian strain isolated in 1992 (O. Kew, personal communication). PV1(LS-a), PV2(L), PV2(MEF-1), and PV2(IND) were a generous gift from O. Kew (CDC, Atlanta, GA, U.S.A) PV1(VP1–54) is a strain we constructed by site-directed mutagenesis.[38] This strain, originally described to be mouse neurovirulent[21] carries a single amino acid exchange (P1054S) in capsid polypeptide VP1. Prior to use, the titer of each virus sample was determined in a plaque assay.

Transgenic ICR-mice expressing the *h*PVR[10] were a generous gift from A. Nomoto (The University of Tokyo, Japan). Swiss-Webster- and normal ICR-mice were obtained from Taconic (Germantown, NY, U.S.A).

***Ultraviolet (UV) irradiation conditions.*** UV irradiation was performed in a UV-stratalinker (Stratagene, LaJolla, CA, U.S.A) A suspension of PV was irradiated at a distance of ca. 10 cm with an intensity of ca. 3.5 J/m$^2$. Virus was exposed to the irradiation source in ice-cooled plastic dishes at a solution depth of ca. 1mm. The loss of infectivity was confirmed in a plaque assay.

***Poliovirus intracerebral infections.*** Virus preparations were used to infect *tg* or normal mice with the desired input titer by intracerebral inoculation. Mice were anesthetized, and a 25 gauge hypodermic needle was used to inject maximally 30 $\mu$l of virus suspension in Dulbecco's minimal essential medium (DMEM). The point of injection was the middle on the median between the ear pinnacle and the eye. Infected mice were regularly observed for symptoms. None of the treated animals showed any external signs of damage or neurological disturbances in 24 h following injection.

***Tissue processing, sectioning, and staining.*** Affected animals in the final stage of their disease were sacrificed according to approved protocols, and their bodies were immediately perfused with 15 ml of phosphate buffered saline (PBS), followed by 15 ml of 4% neutral buffered paraformaldehyde. The brain and spinal cord were removed and fixed for 2 h at room temperature in the fixative used for perfusion. Tissue specimens were rinsed for 30 min in ice-cold PBS, then placed in 70% ethanol over night. Dehydration was achieved through a scheme of gradually increasing ethanol concentration, followed by clearing in toluene for 2 h and infiltration with paraffin at 57.5 °C for 2 h. Neural tissues were embedded and cut on a rotary microtome at a thickness of 10 $\mu$m. Tissue sections were placed on microscopic slides treated with 3-aminopropyltriethoxysilane (Sigma, St. Louis, MO, U.S.A.) and dried overnight. For staining, sections were deparaffinized in xylene and rehydrated in sequential ethanol solutions

**Table 1** Experimental infections of *h*PVR-*tg*- and Swiss-Webster-mice with different PV strains

| PV strain used | PFU inoculated intracerebrally | Latency period* | Pathological picture | Fatalities/ infected mice† |
|---|---|---|---|---|
| *h*PVR-*tg* mice | | | | |
| PVI(M) | $1 \times 10^4$ | 2–5d. | poliomyelitis | 4/4 |
| | $1 \times 10^5$ | 48–72 hrs. | | 4/4 |
| | $5 \times 10^6$ | 24–48 hrs. | | 4/4 |
| PV2(MEF-1) | $1 \times 10^4$ | 2–5d. | polioencephalomy-elitis | 4/4 |
| PV2(L) | $1 \times 10^4$ | 2–5d. | polioencephalomy-elitis | 4/4 |
| PV1(LS-a) | $1 \times 10^4$ | 2–5 < et < btd. | poliomyelitis | 4/4 |
| Normal mice | | | | |
| PV1(M) | $5 \times 10^6$ | – | – | 0/12 |
| PV2(MEF-1) | $1 \times 10^4$ | 3–5 d. | diffuse | 2/4 |
| | $1 \times 10^5$ | 3–4 d. | encephalomyelitis | 2/4 |
| | $5 \times 10^6$ | 2–3 d. | | 4/4 |
| PV2(IND) | $5 \times 10^6$ | 2–3 d. | diffuse encephalomyelitis | 4/4 |
| PV2(L) | $5 \times 10^6$ | 3–5 d. | diffuse encephalomyelitis | 9/12 |
| PV2(W2) | $5 \times 10^6$ | 6–14 d. | diffuse encephalomyelitis | 5/8 |
| PV1(LS-a) | $1 \times 10^5$ | 5–10d. | panmyelitis | 0/10 |
| | $5 \times 10^6$ | 4–7 d. | | 0/10 |
| PV1(VP1–54) | $< 1 \times 10^9$ | – | – | 0/8 |
| | $1 \times 10^9$ | 3–5d. | encephalomyelitis | 4/8 |

* Latency period from time of inoculation until appearance of initial symptoms.

† The duration of the clinical course from onset of symptoms until death was uniformly 36–48 h in *h*PVR-*tg* animals. The time course of infection in mice with diffuse encephalomyelitis was highly variable, even within the group of animals infected with the same PV isolate.

of decreasing concentration. Toluidine blue and luxol fast blue, periodic acid Schiff (PAS), hematoxylin stainings were performed according to standard procedures.[42]

***Immunohistochemistry.*** Rabbit polyclonal anti-PV2(L) antisera were produced as described elsewhere.[43] The IgG fraction was isolated from the polyclonal serum via a protein A-sepharose column (Pharmacia, Sweden).

Paraffin-embedded 8 $\mu$m thick sections of brain and spinal cord were deparaffinized in toluene, rehydrated in graded ethanol and rinsed through PBS once. Rehydrated sections were placed in a damp chamber and blocked with 3% normal goat serum in PBS for 30 min. After removal of the blocking solution, anti-PV2(L) polyclonal antiserum was applied at a dilution of 1:200, 1:500, or 1:1000 in PBS. After three rounds of washing in PBS, biotin labeled anti-rabbit IgG (Sigma, St. Louis, MO, U.S.A.) — preadsorbed with 2% mouse serum — was applied at a concentration of 1:200 in PBS for 1 h. Afterwards, sections were washed three times with PBS and Avidin-FITC complex (Sigma, St. Louis, MO, U.S.A.) was used at a concentration of 1:100 in PBS to treat sections for 30 min. Following three washing steps in PBS, sections were mounted with vectastain (Vector Lab, Burlingame, CA, U.S.A.).

## Results

### *hPVR-tg mice infected with PV1(M)*

Transgenic mice expressing the PV receptor[10] were infected intracerebrally with PV1(M) with an amount of virus ranging from $10^4$ to $5 \times 10^6$ plaque forming units (PFU). All infected mice developed a characteristic neurological syndrome displaying stereotypic clinical features irrespective of input titer of virus and differing only with regard to onset of symptoms (Table 1). Once visible signs of functional impairment were apparent, the progression of disease followed a predictable course. Two to five

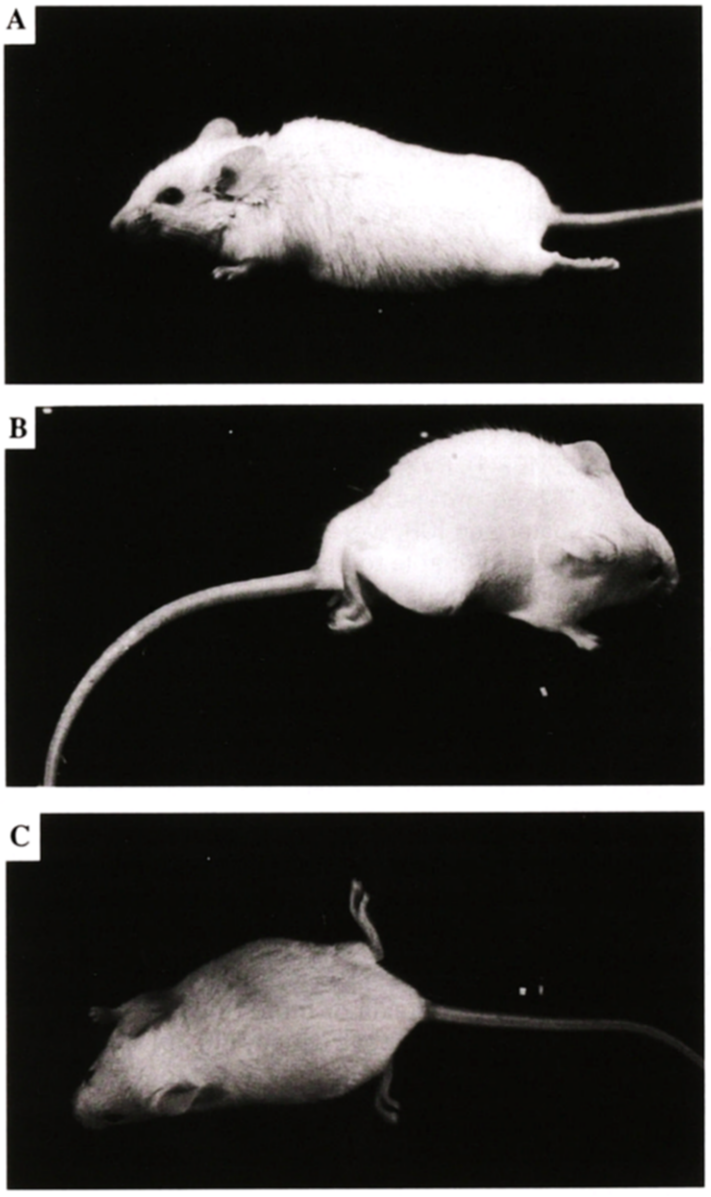


**Fig. 1.** (A–C). Clinical appearance of PV-infected *h*PVR-*tg*- (A) and normal ICR-mice (B and C). (A) Typical habitus of *h*PVR-*tg* mice with flaccid paraparesis 72 h p.i. with PV1(M). (B). Kyphoscoliosis in a normal mouse infected with PV2(MEF-1) 4 days p.i. Note the 'claw' deformity, due to spastic paresis of the right lower extremity. (C) A non-transgenic mouse with spastic paraparesis. The animal was photographed one week after infection with PV1(LS-a).

days after intracerebral injection, initial signs were invariably a flaccid paralysis of the lower extremities and tail (Fig. 1A). The condition was rapidly progressive leading to complete immobilization and respiratory difficulty within 48 h. Respiratory distress caused visible signs of bobbing of the head, strenuous respiratory effort, insufficient thoracic excursions, and nasal flaring. Animals in the final stage of the disease were killed and their CNS tissues processed according to standard procedures.

Histopathological analysis of the CNS of PV1(M)-infected *h*PVR-*tg* mice revealed

the spinal pathology of poliomyelitis described in earlier reports.[10,11] Selective loss of anterior horn motor neurons along the entire spinal cord was invariably present (Fig. 2B). Foci of virally-induced damage in the higher cervical cord extended into the brain stem and were accompanied by minor signs of inflammation in a predominantly perivascular distribution. Characteristically, apart from a clearly defined lesion in the pyramidal cell layer of the hippocampal formation, lesions above the brain stem were absent in all cases analyzed. The appearance of initial lesions in the lumbar spine, distant from the injection site without evidence of damage to cortical motor neurons or descending tracts, indicated that virus had been disseminated via the hematogenous or cerebrospinal fluid route.

***Intracerebral infection of normal mice with PV1(M) and PV2-related strains***

Twenty eight day old Swiss-Webster- and ICR-mice were injected intracerebrally with PV1(M), PV2(L), PV2(MEF-1), PV2(IND), or PV2(W2), with amounts of virus ranging from $10^4$ to $5 \times 10^6$. Three groups of four animals each with different genetic backgrounds, Swiss-Webster and ICR, were injected with the same viral strain. It is important to note that we were unable to detect clinical or histological evidence for differences in susceptibility towards PV infection between both outbred mouse strains used. Therefore, in the following text, the term 'normal mouse' will refer to Swiss-Webster mice. All *mn* PV strains assayed caused poliomyelitis when injected into *h*PVR-*tg* mice (clinical and histopathological details are described later). None of the normal mice injected with PV1(M) showed clinical signs of neurological damage, whereas inoculation of type 2 PV strains produced signs of CNS infection (Table 2).

Mice infected with PV2(MEF-1) and PV2(IND) were most severely affected. Initial symptoms appeared 2–5 days post infection (p.i.) in all animals but they were inconsistent regarding the sites of manifestation and quality of functional impairment. Motor symptoms consisted predominantly of spastic weakness involving the lower or upper extremities in a random fashion (Table 2). Paraplegic animals had a characteristic posture marked by kyphoscoliotic deformity (Fig. 1B). The progression of motor symptoms did not follow any apparent topographical scheme. Pareses frequently were accompanied by gait ataxia or motor incoordination. Clinical signs of respiratory involvement as described above usually did not appear during the course of the disease (Table 2). The clinical course proceeded to a terminal stage within 4 days after onset of symptoms. Preterminal animals were severely emaciated once functional impairment supervened, and refused intake of fluid and food offered within their reach.

Compared to PV2(MEF-1) and PV2(IND) a proportionally lower number of PV2(L)-infected animals died (Table 1). Their clinical syndrome was less variable, but also diverged from the regular pattern of disease localization and progression seen in poliomyelitic *h*PVR-*tg* mice. Motor symptoms similar to those in PV2(MEF-1) infected littermates dominated the clinical picture. Progression of motor involvement did not follow any recognizable pattern and it only rarely included respiratory function (Table 2). Eventually immobilization led to quick deterioration of the starving animals.

PV2(W2) was previously reported to be of attenuated neuropathogenicity with respect to PV2(L) in mice.[44] Accordingly, the proportion of infected animals that developed disease, and the severity and pace of progression of symptoms, were less than in animals infected with other PV type 2 isolates (Table 1). This observation confirms the attenuated nature of the strain.[44] The spectrum of functional deficits observed was identical to PV2(L)-induced disease. Likewise, there was considerable variability in the sites involved in production of symptoms, course of progression,

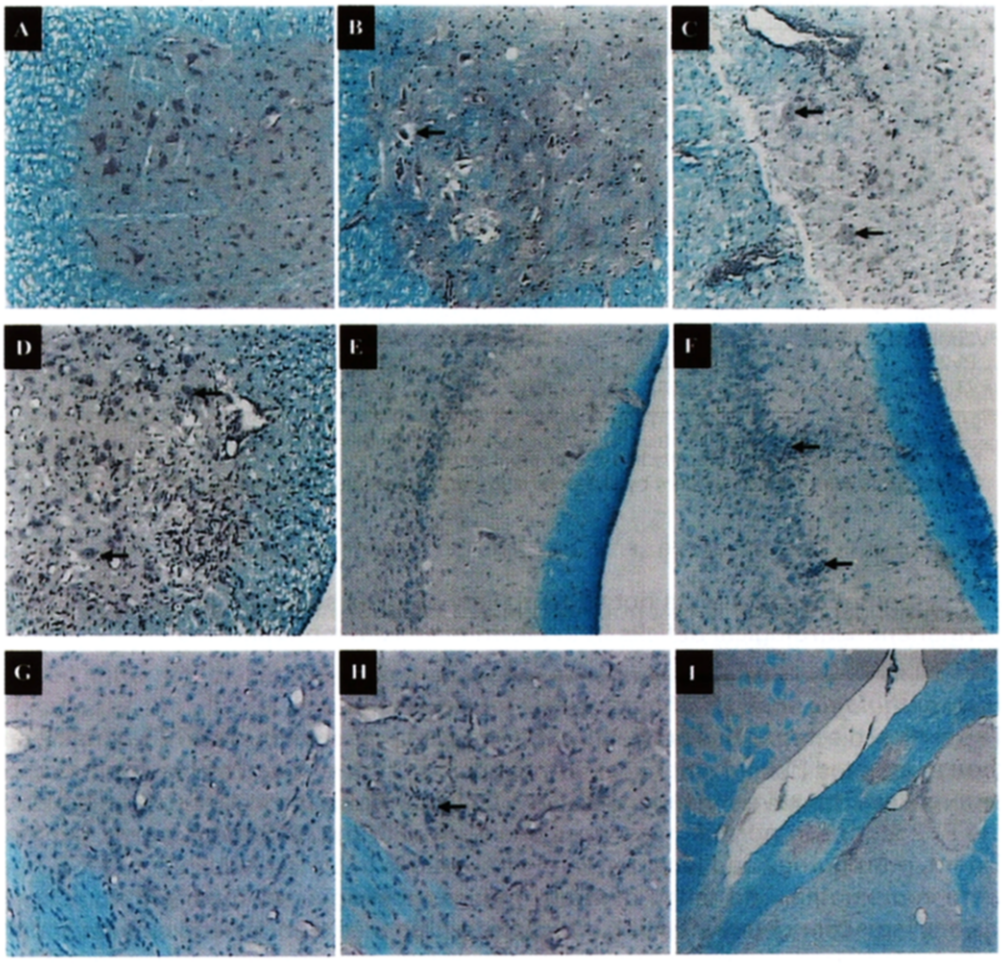

**Fig 2.** (A–1). Histopathology of murine PV infections. *h*PVR-*tg* mice infected with PV1(M) (B, E and G), or normal mice inoculated with PV2(MEF-1) (C, D, F, H and I), were killed 5 days p.i. in a terminal stage of disease, and their neural tissue processed as described. Sections of 10 $\mu$m thickness were stained with luxol fast blue, PAS and hematoxylin. (A). Transverse section through the intact murine spinal cord. The section shows the anterior horn with a prominent group of motor neurons (36 ×) (B). Transverse section through the cervical spinal cord of a *h*PVR-*tg* mouse after infection with PV1(M). Motor neurons with different stages of cytopathological damage are seen within the anterior horn, a necrolytic neuron is indicated by an arrow. Neurons in posterior parts of the spinal cord were preserved and infiltrative changes were moderate (36 ×) (C). Transverse section through the cervical spinal cord of a normal mouse infected with PV2(L). Perivascular infiltrates invaded the spinal white and gray matter, but motor neurons (marked by arrows) appeared intact (36 ×).(D). Section through an adjacent area of (C) with diffuse infiltrations show neuronal destruction within the gray matter, and microglial proliferation in the white and gray matter. As in (C) intact motor neurons can be distinguished within areas of structural alteration (arrows) (36 ×). (E) The insular cortex of a *h*PVR-*tg* mouse after infection with PV1(M) appears normal (42 ×). (F) Transverse section through the insular cortex of a normal mouse p.i. with PV2(MEF-1). Transcortical microglial nodules (arrows) accompanied neuronal destruction within the cortical neuronal layers. Similar lesions were scattered throughout the cortex (42 ×). (G) The subthalamic nucleus from a PV1(M)-infected *h*PVR-*tg* mouse without pathological changes (42 ×). (H) A section taken from the subthalamic nucleus of a normal mouse after infection with PV2(MEF-1) reveals a microglial nodule, neuronal destruction and perivascular cuffing within the area (42 ×). (I) Two delineated areas of infiltration, rarefaction necrosis and demyelination within the fimbria of a normal mouse infected with PV2(MEF-1). (16 ×). Reproduced here at 65%.

**Table 2** Clinical Symptoms of *h*PVR-*tg*- and normal mice after infection with different PV strains*,†

| PV strain used | Flaccid paraparesis | Spastic limb pareses | Respiratory distress‡ | Kyphoscoliosis | Ataxic gait | Extrapyramidal signs |
|---|---|---|---|---|---|---|
| *h*PVR-*tg* mice | | | | | | |
| PV2(M) | 12/12 | – | 12/12 | – | – | – |
| PV2(MEF-1) | 4/4 | – | 4/4 | – | 2/4 | 1/4 |
| PV2(L) | 4/4 | – | 4/4 | – | – | – |
| PV1 (LS-a) | 4/4 | – | 4/4 | – | – | – |
| normal mice | | | | | | |
| PV1 (M) | – | – | – | – | – | – |
| PV2(MEF-1) | – | 10/12 | 1/12 | 10/12 | 3/12 | 2/12 |
| PV2(L) | – | 9/12 | 2/12 | 9/12 | 1/12 | 0/12 |
| PV1(LS-a) | – | 12/12 | 0/12 | 8/12 | 0/12 | 0/12 |

* Symptomatic/Infected animals
† Animals were assessed clinically in a preterminal stage
‡ Respiratory distress was evident by characteristic signs mentioned in the text

and symptom clusters (data not shown). Few animals survived, and remained with permanent neurological deficits in the form of spastic monopareses.

***Histopathologic analysis of murine PV2 infections***

The clinical discrepancies between *wt* PV-induced poliomyelitis in *h*PVR-*tg* mice, and mouse-adapted PV2 infections in normal mice, were confirmed by histopathological differences. The severity and variability of clinical signs secondary to infection with the PV2 strains in normal mice was consistent with the histopathological findings. Extent, morphology and localization of viral lesions in Swiss-Webster- and ICR-mice were comparable. The range of virally-induced damage encompassed a variety of lesions indiscriminately affecting structures within the cerebral hemispheres and the entire spinal cord. Characteristically, spinal pathology was patchy and irregular, and it did not follow the consistent pattern of damage to the entire cord seen in PV-infected *h*PVR-*tg* mice. Unexpectedly, anterior horn motor neurons remained frequently unaffected in normal mice infected with *mn* PV2, although severe pathological changes within the spinal cord were apparent (Fig. 2C,D). In contrast, murine poliomyelitis in *h*PVR-*tg* mice invariably led to complete and exclusive elimination of the motor neuron population in the spinal cord with only minor infiltrative changes (Fig. 2B). Unlike the limitation of virally-induced lesions in PV infections of *h*PVR-*tg* mice to the spinal cord, PV2-induced disease involved the entire CNS. Microglial nodules accompanied by mixed lymphocytic and neutrophilic infiltrates were scattered throughout the brain and were found within the insular, piriform and temporal cortex (Fig. 2F), and the basal ganglia and thalamus (Fig. 2H). These structures were never affected in infected *h*PVR-*tg* mice (Fig. 2E,G). Perivascular cuffing and dense infiltration of perivascular and periventricular parenchyma were distributed ubiquitously in the CNS. The cerebral white matter was a frequent site of viral lesions. Lymphocytic infiltrates within the cerebral or cerebellar peduncles, the internal capsule, or the long descending tracts and posterior columns within the upper cervical cord, occasionally caused rarefaction necrosis with secondary demyelination (Fig. 2I). Immunohistochemical staining for viral proteins with a polyclonal anti-PV2 antiserum revealed positive signals in those structures frequently involved by virally-

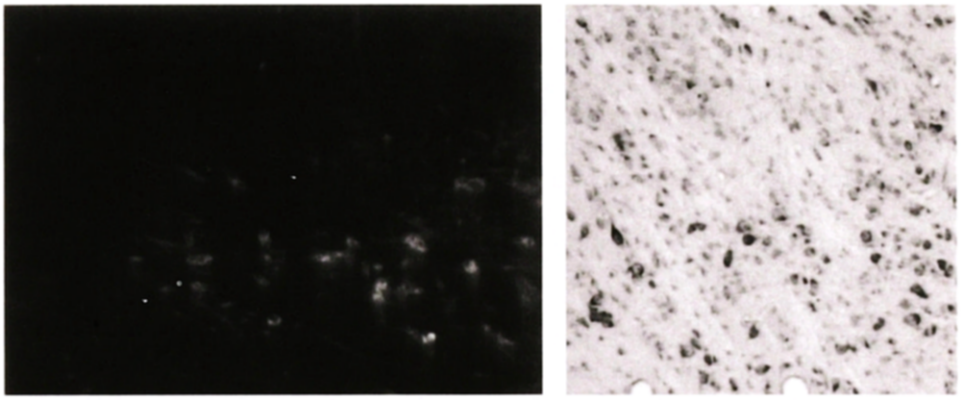

**Fig. 3.** Immunohistochemical staining with an anti-PV2 polyclonal antiserum. A transverse section from the brain of a Swiss-Webster mouse 4 days p.i. with PV2(MEF-1) was treated as described in Materials and Methods. A group of cortical neurons within the frontal cortex stains positively for viral protein. The right hand image shows the same area in a neighboring section stained with toluidine blue (32x). Reproduced here at 65%.

induced lesions. A group of frontal cortical neurons, expressing viral proteins is shown in Fig. 3.

Signs of widespread lesions and diffuse encephalomyelitis were most commonly associated with the isolates PV2(MEF-1) and PV2(IND), whereas in PV2(L) cases a myelitic pattern of disease predominated over encephalitis.

Parallel to the clinical findings, overall CNS damage induced by PV2(W2) was moderate in comparison with the other serotype 2 isolates. Neurological damage focused on the spinal cord with rare cerebral involvement. Spinal pathology qualitatively resembled the PV2 panmyelitis described above but the extent and number of lesions were reduced (data not shown).

### *Infection of h*PVR-*tg* mice with PV2 strains

To analyze the clinical course of murine infection with PV2 in mice expressing the *h*PVR, *tg* mice were inoculated intracerebrally with PV2(MEF-1) or PV2(L). The resulting clinical picture featured signs typically seen in murine poliomyelitis. The onset of disease was marked by a flaccid paraparesis, followed by ascending progressive symptoms as in poliomyelitis. All affected animals developed a preterminal dyspneic stage before they were killed.

Associated histopathology showed elements characteristic of *h*PVR-mediated poliomyelitis, as well as PV2-induced encephalomyelitis. Anterior horn motor neurons had changes typical for poliomyelitis. In addition, there was almost always severe hemispheric involvement, never associated with *h*PVR-*tg* murine poliomyelitis resulting from infection with PV1(M). Lesions equivalent to those seen in PV2-induced encephalomyelitis were distributed in the same widespread indiscriminate manner throughout the CNS. Gray matter structures were affected as well as cerebral white matter (data not shown).

### *Intracerebral infection of non-transgenic mice with PV1 (LS-a)*

Two groups of ten 28-day-old Swiss-Webster- and ICR- mice were each infected intracerebrally with PV1(LS-a) at a range of $10^5$ to $5 \times 10^6$PFU. As in previous assays, there was no notable difference in clinical signs and histopathological features in mice with different genetic background. All infected animals developed a specific neurological syndrome with stereotypical onset, clinical course, functional deficits,

and pattern of progression. Four days p.i., mice showed the first signs of an insidious spastic paraparesis (Fig. 1C). No ascending motor deficits occurred, respiratory function remained unaffected, and there were no fatalities. Intracerebral inoculation of PV1(LS-a) was required to produce symptoms, since intravenous injection of virus with concomitant intracerebral needle puncture produced no neurological impairment. Intracerebral inoculation of equal particle numbers of PV1(LS-a) virus, inactivated by UV-irradiation, also caused no neurological signs of CNS damage. This finding indicated viral replication to be a prerequisite for PV1(LS-a) neuropathogenicity. Histopathology of the neurological syndrome caused by this variant centered exclusively on the spinal cord. Extensive infiltrates, originating from spinal blood vessels, invaded both the gray and white matter. Pathologic changes involved the entire spinal cord, but did increase in extent of damage caudally (Fig. 4A,B). There was no apparent predilection for any cell subtype. Motor neuron damage was seen within areas of destructive necrotic tissue change secondary to the inflammation. At no time during the infection could damage to motor neurons within the thoracic or cervical cord be distinguished (Fig. 4B), despite prominent inflammation affecting these regions. Spinal sections taken from animals which underwent partial reversal of neurological defects, 4 weeks p.i., revealed complete regression of infiltrative changes and preservation of motor neuron populations (Fig. 4C).

***Intracerebral infection of normal mice with PV1(VP1–54)***

A mutant PV1(M) virus, which had previously been reported to exert neuropathogenic potential in normal mice[21] was tested in a similar manner as the above mentioned strains. PV1(VP1–54) carried a point mutation at position 54 (P1054S) within capsid protein VP1. Intracerebral inoculation of each four Swiss-Webster- and ICR-mice with at least $1 \times 10^9$PFU resulted in visible signs of neurological damage in 50% of affected animals in both groups. With the genetic variant constructed in this laboratory, this large inoculum was required to induce clinical signs. The nature of the neurological syndrome was partly obfuscated by the vigorous host response to the application of excess viral antigen, and the resulting clinical deterioration. Sick mice showed prominent systemic signs of disease such as ruffled fur, reduced activity, and emaciation. Symptoms of minor motor impairment were present in half of the diseased mice, but the limb pareses were difficult to assess in quality due to the general weakened state of the animal. Mild limb weakness did not progress with any apparent disease pattern. Severely weakened, emaciated animals succumbed to the effects of infection, without the clear causal relationship of neurological disease and fatal outcome seen in poliomyelitis. *h*PVR-*tg* mice injected with PV1(VP1–54) developed a neurological condition indistinguishable from PV1(M) related poliomyelitis (data not shown). Similar to clinical findings, the histopathologic features induced by PV1(VP1–54) were less defined than in the other described infections. There was no supraspinal involvement, and spinal cord sections at all levels displayed widespread parenchymal invasion and reactive migroglial proliferation. No targeted attack against specific cell populations was apparent (Fig. 4D). Histopathologic evidence for a primary thoracic and cervical cord affection was not present.

## Discussion

With the rare exception of certain serotype 2 PV strains, e.g. PV2(MEF-1) and PV2(L), naturally occurring PV strains can only infect primates, and even PV2(MEF-1) and PV2(L) are mouse neurovirulent only when artificially inoculated by intracerebral injection. The narrow host range of PV results from its stringent dependence on the

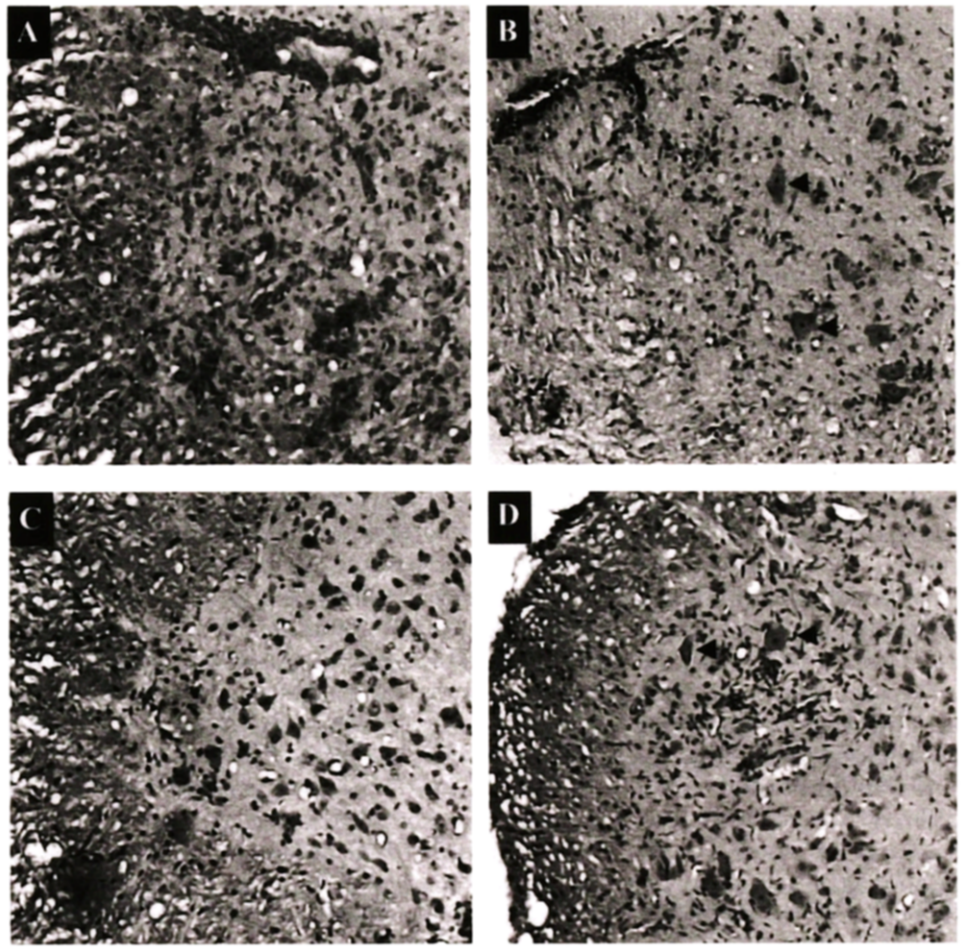


**Fig. 4.** (A–D) Transverse sections through the spinal anterior horn of normal mice infected with PV1(LS-a) (A–C) or PV1(VP1-54) (D) (36×). (A) Lumbar spinal cord, 5 days p.i. Dense infiltrates, centering around spinal vessels, invade the surrounding spinal gray and white matter. Motor neuron populations occasionally were affected by severe infiltrative changes in the spinal gray matter, but selective attack on this group of neurons was not evident. (B) Cervical spinal cord of the same case as in A. Infiltrates of similar morphology and distribution are confined to the perivascular regions. Damage to anterior horn motor neurons was absent (arrowheads), in spite of widespread infiltrative changes within the spinal white matter in the thoraco-cervical segments. (C) Lumbar spinal cord of a normal mouse 30 days p.i. with PV1(LS-a). In parallel with clinical remission, most areas of infiltration were cleared, and anterior horn motor neurons remained intact. (D) Cervical spinal cord 5 days p.i. with PV(VP1-54). Diffuse microglial proliferation and predominantly neutrophilic infiltration affected the entire section through the spinal cord at all levels. Selective injury to motor neurons did not occur (arrowheads point toward intact motor neurons). Reproduced here at 75%.

poliovirus receptor (*h*PVR and the closely related monkey homologue, *m*PVR), an Ig-like cell surface molecule expressed only by primate cells.[8] The murine homologue to *h*PVR cannot function as PV receptor,[13] as expected. All mouse adapted PVs have been selected for a neurovirulent phenotype (*mn*), hence, they have acquired the ability to proliferate in the murine CNS. Significantly, these *mn* PV strains cannot interact with the mouse homologue of *h*PVR either; in fact, none of the *mn* PV strains can infect mouse tissue cells in culture. *Mn* PV strains must, therefore, use pathway(s) to enter cells of the mouse CNS that involve receptors distinct from the mouse homologue of *h*PVR. These considerations render the possibility that *mn* PVs would

express exactly the same cell tropism in the murine CNS as they do in the primate CNS unlikely and, hence, that *mn* PVs would cause the same specific disease syndrome (poliomyelitis) in normal mice as they do in primates. To shed some light on these complex problems we have compared the disease syndromes caused by a variety of different PV strains in *h*PVR-*tg* and normal mice. We have come to the conclusion that *mn* PV strains do not produce poliomyelitis in normal mice.

The occurrence of poliomyelitis in *h*PVR-*tg* mice corroborates the function of the *h*PVR as a major determining factor in the pathogenesis of the peculiar histopathological and clinical features of this disease.[10,11] Poliomyelitis in *tg* mice followed a stereotypic course: initial flaccid pareses of the lower limbs, followed by cranial progression, involving respiratory function, and fatal outcome. In contrast, the clinical symptoms resulting from *mn* PV infections in normal Swiss-Webster-and ICR-mice could not be explained by classical terms of the syndrome poliomyelitis. Infection of normal mice with *mn* PV strains caused a diffuse encephalomyelitis with highly variable neurological symptoms appearing in random order, at topographically unrelated sites. Mouse neuropathogenicity was shared by several serotype 2 field isolates, the mouse adapted attenuated strain PV2(W2), the PV1(M) derivative PV1(LS-a), and PV1(M) with a mutation in residue 54 of capsid protein VP1. Interestingly, the type 2 PV field isolates PV2(MEF-1) and PV2(IND), have been reported to be *mn* without a lengthy process of adaptation, whereas other type 2 [PV2(L)] and type 1 strains [PV1(LS-a)] were passaged in the rodent CNS before they acquired the *mn* phenotype. *Mn* type 1 or type 3 PV field isolates have not been described. The molecular basis underlying this peculiar property of type 2 PV strains is not understood.

Earlier reports stressed the similarity between primate poliomyelitis and encephalomyelitis caused by PV2(L) in normal mice.[16] Comparative studies at that time were impeded by the lack of a murine model of *h*PVR-mediated poliomyelitis. Viral antigen was shown to be expressed in spinal anterior horn motor neurons,[16] but *in situ* hybridization revealed the presence of viral RNA in cells in posterior portions of the spinal cord as well as the white matter.[45]

Previous analyses of PV neurovirulence using *mn* strains were based on the assumption of a similar pathogenesis of *mn* PV infections in *wt* mice and in primates. One parameter to assess the potential of viral neurovirulence is the $LD_{50}$ value, and in earlier studies, animals showing evidence of neurological functional impairment were generally killed without further histopathological analysis (see for example, ref. 17). Our results suggest that the expression of the *mn* phenotype of PV strains in mice should not be compared to the expression of PV neurovirulence in primates, the normal host. Indeed, it appears that the expression of a *mn* phenotype in *wt* mice can result from very different genetic changes in PV strains, and that each genetic change can produce different syndromes. This is apparent not only from various type 2 *mn* strains, but also from the type 1 *mn* strain PV1(LS-a) [a derivative of PV1(M) whose genotype has been recently elucidated[38]]. Histopathological changes within the CNS should therefore be monitored when murine infections with *mn* PV strains are studied.

A major determinant for the *mn* phenotype of PV2(L) is the BC-loop of VP1[17] a surface protrusion of about 10 amino acids located at the apex of the poliovirion[46] that functions as a neutralization antigenic site.[47] Exchange of the VP1 BC-loop of the mouse-inert PV1(M) with the BC-loop of PV2(L) produces the *mn* phenotype,[18,19] an observation that prompted speculation that the VP1 BC-loop is involved in the recognition of a putative mouse receptor. No evidence for this hypothesis has been obtained as yet.

Strain PV1(LS-a), a *mn* derivative of PV1(M), accumulated 54 point mutations during passage in non-human tissue, of which 10 mutations led to amino acid exchanges in the capsid region.[38] These capsid mutations, however, were insufficient to produce the *mn* phenotype. Instead, the mutations in capsid protein VP1 plus, surprisingly, five mutations in the coding region of the non-structural protein $2A^{pro}$, a proteinase, produced mouse neurovirulence. The syndrome PV1 (LS-a) induced in normal mice, however is distinct from the encephalomyelitis caused by type 2 PV strains.

A pathological entity different from those observed with all other *mn* poliovirus strains, was seen with PV1(VP1-54), a virus that we constructed according to a previous report.[21] PV1(VP1–54) is a *mn* derivative of PV1(M) that carries only a single amino acid exchange in capsid protein VP1 (P1054S). The mutation, located at an interpentameric interface inside the capsid, was suggested to destabilize the virion in the mouse CNS, but the neurological syndrome caused by infection with PV1(VP1-54) was not histopathologically characterized.[21] Infection of mice with PV1(VP1-54) led to neurological damage only after intracerebral inoculation of excess viral antigen. The poorly defined histopathological features of CNS involvement lacked characteristics of specificity observed in *h*PVR-mediated poliomyelitis.

The genotypic differences between *mn* PV strains and the clinical syndromes they cause, which differ from *h*PVR-mediated poliomyelitis, challenge the hypothesis of common determinants of a *mn* phenotype. Rather, it appears that a multitude of non-related genetic elements affect this phenotypic marker in various ways. As indicated before, the nature of the receptor(s) used by the *mn* PV strains in the mouse CNS remains to be determined. Available data suggest that the mouse homologue to the *h*PVR does not serve as surrogate for the *mn* PV strains.[13] It is more likely that the *mn* PV strains enter neuronal tissue via cell-surface protein(s) unrelated to *h*PVR. If so, it is not surprising that the syndromes produced by these viral strains are distinct from poliomyelitis.

In recent years picornaviruses other than poliovirus have been implicated as causative agents of neurological disease. These include enterovirus (EV) 70,[48] the etiologic agent of acute hemorrhagic conjunctivitis, or EV 71.[49] However, it has also been reported that the encephalomyelitis caused by the newly emerging human pathogen EV 71 did not always resemble poliomyelitis.[50] The evolution of enterovirus strains with new neuropathogenic properties distinct from previously non-neuropathogenic ancestors might be due to adaptation to new receptor entities. The mouse-neurotropic PV variants with altered cell tropism constitute a precedent for the emergence of non-poliomyelitic picornaviral CNS disease.

We thank A. Nomoto for the generous gift of the *h*PVR-*tg* mouse strain used in this study and B. Jubelt and O. Kew for kindly providing PV type 2 strains. We are grateful to P. Coyle for critical review of this manuscript. We thank N. Peress for helpful discussion and D. Colflesh for help with microscopic imaging. This work was supported in part by NCI grant CA28146, and NIH grants AI15122 and AI32100. M.G. is a recipient of a grant from the Stipendienprogramm Infektionsforschung, Heidelberg, Germany.

## References

1. Sicinski P, Rowinski J, Warchol JB *et al.* Poliovirus type 1 enters the human host through intestinal M cells. Gastroenterology 1990; 98: 56–8.
2. Bodian D. Emerging concept of poliomyelitis infection. Science 1955; 122: 105–8.

3. Blinzinger K, Simon J, Magrath D, Boulger L. Poliovirus crystals within the endoplasmic reticulum of endothelial and mononuclear cells in the monkey spinal cord. Science 1969; 163: 1336–7.
4. Bodian D. Poliomyelitis. p. 2323–2344. In: Minckler J, ed. Pathology of the Nervous System, vol. 3. New York: McGraw-Hill, 1972: 2323–44.
5. Kojima H, Furuta Y, Fujita M, Fujioka Y, Nagashima K. Onuf's motoneuron is resistant to poliovirus. J Neurol Sci 1989; 93: 85–92.
6. Koike S, Horie H, Ise *et al.* The poliovirus receptor protein is produced both as membrane-bound and secreted forms. EMBO J 1990; 9: 3217–24.
7. Mendelsohn CL, Wimmer E, Racaniello VR. Cellular receptor for poliovirus: Molecular cloning, nucleotide sequence, and expression of a new member of the immunoglobulin superfamily. Cell 1989; 56: 855–65.
8. Wimmer E, Harber JJ, Bibb JA, Gromeier M, Lu HH, Bernhardt G. The poliovirus receptors. In: Wimmer E, ed. Cellular Receptors for Animal Viruses. Cold Spring Harbor, NY: Cold Spring Harbor Press 1994, *in press.*
9. Bernhardt G, Bibb JA, Bradley J, Wimmer E. Molecular characterization of the cellular receptor for poliovirus. Virology 1994; 199: 105–13.
10. Koike S, Taya C, Kurata T, Abe S, Ise I, Yonekawa H, Nomoto A. Transgenic mice susceptible to poliovirus. Proc Natl Acad Sci USA 1991; 88: 951–5.
11. Ren R, Costantini F, Gorgacz EJ, Lee JJ, Racaniello VR. Transgenic mice expressing a human poliovirus receptor: a new model for poliomyelitis. Cell 1990; 63: 353–62.
12. Koike S, Ise I, Sato H, Yonekawa H, Gotoh O, Nomoto A. A second gene for the african green monkey poliovirus receptor that has no putative N-glycosylation site in the functional N-terminal immunoglobulin-like domain. J Virol 1992; 66: 7059–66.
13. Morrison ME, Racaniello VR. Molecular cloning and expression of a murine homolog of the human poliovirus receptor gene. J Virol 1992; 66: 2807–13.
14. Armstrong C. The experimental transmission of poliomyelitis to the eastern cotton rat, *Sigmodon hispidus hispidus.* Public Health Rep 1939a; 54: 1719–21.
15. Armstrong C. Successful transfer of the Lansing strain of poliomyelitis virus from the cotton rat to the white mouse. Public Health Rep 1939b; 54: 2302–5.
16. Jubelt B, Gallez-Hawkins G, Narayan O, Johnson RT. Pathogenesis of human poliovirus infection in mice. I. Clinical and pathological studies. J Neuropathol Exp Neurol 1980; 39: 138–49.
17. LaMonica N, Meriam C, Racaniello VR. Mapping of sequences required for mouse neurovirulence of poliovirus type 2 Lansing. J Virol 1986; 57: 515–25.
18. Martin A, Wychowski C, Couderc T, Crainic R, Hogle J, Girard M. Engineering a poliovirus type 2 antigenic site on a type 1 capsid results in a chimaeric virus which is neurovirulent for mice. EMBO J 1988; 7: 2839–47.
19. Murray MG, Bradley J, Yang XF, Wimmer E, Moss EG, Racaniello VR. Poliovirus host range is determined by a short amino acid sequence in neutralization antigenic site I. Science 1988; 241: 213–5.
20. Couderc T, Hogle J, LeBlay H, Horaud F, Blondel B. Molecular characterization of mouse-virulent poliovirus type 1 Mahoney mutants: involvement of residues of polypeptides VP1 and VP2 located on the inner surface of the capsid protein shell. J Virol 1993; 67: 3808–17.
21. Moss EG, Racaniello VR. Host range determinants located on the interior of the poliovirus capsid. EMBO J 1991; 10: 1067–74.
22. Pevear DC, Oh CK, Cunningham LL, Calenoff M, Jubelt B. Localization of genomic regions specific for the attenuated, mouse-adapted poliovirus type 2 strain W-2. J Gen Virol 1990; 71: 43–52.
23. Wimmer E, Hellen CUT, Cao XM. Genetics of Poliovirus. Ann Rev Genet 1993; 27: 353–436.
24. Lustig S, Jackson AC, Hahn CS, Griffin DE, Strauss EG, Strauss JH. Molecular basis of Sindbis Virus neurovirulence in mice. J Virol 1988; 62: 2329–36.
25. Russell DL, Dalrymple JM, Johnston RE. Sindbis virus mutations which coordinately affect glycoprotein processing, penetration, and virulence in mice. J Virol 1989; 63: 1619–29.
26. Glasgow GM, Sheahan BJ, Atkins GJ, Wahlberg JM, Salminen A, Liljestroem P. Two mutations in the envelope glycoprotein E2 of Semliki Forest Virus affecting the maturation and entry patterns of the virus alter pathogenicity for mice. Virology 1991; 185: 741–8.
27. Pletnev AG, Bray M, Lai CJ. Chimeric tick-borne encephalitis and Dengue type 4 viruses: effects of mutations on neurovirulence in mice. J Virol 1993; 67: 4956–63.
28. Kawano H, Rostapshov V, Rosen L, Lai CJ. Genetic determinants of Dengue type 4 virus neurovirulence for mice. J Virol 1993; 67: 6567–75.
29. Li S, Schulman J, Itamura S, Palese P. Glycosylation of neuraminidase determines the neurovirulence of Influenza A/WSN/33 virus. J Virol 1993; 67: 6667–73.
30. Seif I, Coulon P, Rollin PE, Flamand A. Rabies virulence: effect on pathogenicity and sequence characterization of rabies virus mutations affecting antigenic site III of the glycoprotein. J Virol 1985; 53: 926–34.
31. DesGroseillers L, Barette M, Jolicoeur P. Physical mapping of the paralysis-inducing determinant of a wild mouse ecotropic neurotropic virus. J Virol 1984; 52: 356–63.
32. Fazakerley JK, Parker SE, Bloom F, Buchmeier MJ. The V5A13.1 envelope glycoprotein deletion mutant of mouse hepatitis virus type 4 is neuroattenuated by its reduced rate of spread in the central nervous system. Virology 1992; 187: 178–88.

33. Spriggs DR, Bronson RT, Fields BN. Hemagglutinin variants of Reovirus type 3 have altered central nervous system tropism. Science 1983; 220: 505–7.
34. Rodriguez M, Roos RP. Pathogenesis of early and late disease in mice infected with Theiler's virus, using intratypic recombinant GDVII/DA viruses. J Virol 1992; 66: 217–25.
35. Paquette Y, Hanna Z, Savard P, Brousseau R, Robitaille Y, Jolicoeur P. Retrovirus-induced murine motor neuron disease: mapping the determinant of spongiform degeneration within the envelope gene. Proc Natl Acad Sci USA 1989; 86: 3896–3900.
36. Tyler KL, Bronson RT, Brandt Byers K, Fields B. Molecular basis of viral neurotropism. Neurology 1985; 35: 88–92.
37. Li CP, Schaeffer M. Isolation of a non-neurotropic variant of type 1 poliomyelitis virus. Proc Soc Exp Biol Med 1954; 87: 148–53.
38. Lu HH, Yang CF, Murdin AD, Harber JJ, Kew OM, Wimmer E. Mouse-neurovirulence determinants of poliovirus type 1 strain LS-a map to the coding regions of capsid protein VP1 and proteinase $2A^{Pro}$. J Virol 1994; 68: 7507–15.
39. Koprowski H, Norton TW, Jervis GA. Studies on rodent adapted poliomyelitis virus. I. Cerebral resistance induced in the rhesus monkey. Bacteriological Proceedings 1951; 24: 92.
40. Schlesinger RW, Morgan JM, Olitsky PK. Transmission to rodents of Lansing type poliomyelitis virus originating in the Middle East. Science 1943; 98: 452–4.
41. Van Prooijen-Knegt AC, Van Hoek JFM, Bauman JGJ, Van Duijn P, Wool IG, Van der Ploeg M. In situ hybridization of DNA sequences in human metaphase chromosomes visualized by an indirect fluorescent immunocytochemical procedure. Exp Cell Res 1982; 141: 397–407.
42. Luna LG. Manual of Histological Staining Methods of the American Armed Forces Institute of Pathology, 3rd edn. New York: Mc Graw-Hill, 1968.
43. Murdin AD, Lu HH, Murray MG, Wimmer E. Poliovirus antigenic hybrids simultaneously expressing antigenic determinants from all three serotypes. J Gen Virol 1992; 73: 607–11.
44. Jubelt B, Meagher JB. Poliovirus infection of cyclophosphamide-treated mice results in persistence and late paralysis: I. Clinical, pathologic, and immunologic studies. Neurology 1984; 34: 486–93.
45. Couderc T, Guinguene B, Horaud F, Aubert–Combioscu A, Crainic R. Molecular pathogenesis of type 2 poliovirus in mice. Eur J Epidemiol 1989; 5: 270–3.
46. Hogle JM, Chow M, Filman DJ. The three-dimensional structure of poliovirus at 2.9 Å resolution. Science 1985; 229: 1358–65.
47. Minor PD. Antigenic structure of picornaviruses. Curr Top Immunol Microbiol 1990; 161: 121–54.
48. Hung TP, Sung SM, Liang HC, Landsborough D, Green IJ. Radiculomyelitis following acute haemorrhagic conjunctivitis. Brain 1967; 99: 771–90.
49. Schmidt NJ, Lennette EH, Ho HH. An apparently new enterovirus isolated from patients with disease of the central nervous system. J Infect Dis 1974; 129: 304–9.
50. Melnick JL. Enterovirus type 71 infections: a varied clinical pattern sometimes mimicking paralytic poliomyelitis. Rev Infect Dis 1984; 6: S387–90.